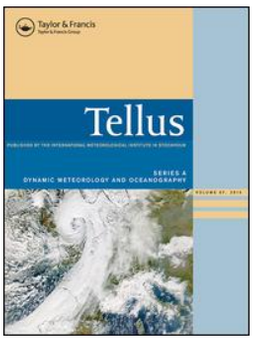

Tellus A: Dynamic Meteorology and Oceanography

ISSN: (Print) 1600-0870 (Online) Journal homepage: https://www.tandfonline.com/loi/zela20

A Global Climatology of Explosive Cyclones using a Multi-Tracking Approach

Marco Reale, Margarida L.R. Liberato, Piero Lionello, Joaquim G. Pinto, Stefano Salon & Sven Ulbrich

To cite this article: Marco Reale, Margarida L.R. Liberato, Piero Lionello, Joaquim G. Pinto, Stefano Salon & Sven Ulbrich (2019) A Global Climatology of Explosive Cyclones using a Multi-Tracking Approach, Tellus A: Dynamic Meteorology and Oceanography, 71:1, 1-19, DOI: 10.1080/16000870.2019.1611340

To link to this article: https://doi.org/10.1080/16000870.2019.1611340

Published online: 24 May 2019.

Tellus SERIES A DYANAMIC METEOROLOGY AND OCEANOGRAPHY
PUBLISHED BY THE INTERNATIONAL METEOROLOGICAL INSTITUTE IN STOCKHOLM

A Global Climatology of Explosive Cyclones using a Multi-Tracking Approach

By MARCO REALE[1,2]*, MARGARIDA L.R. LIBERATO[3,4], PIERO LIONELLO[5,6], JOAQUIM G. PINTO[7], STEFANO SALON[2], and SVEN ULBRICH[8,9], [1]*Abdus Salam ICTP, strada costiera 11, Trieste, Italy;* [2]*Istituto di Oceanografia e di Geofisica Sperimentale - OGS, Via Beirut 2-4, Trieste;* [3]*Universidade de Trás-os-Montes e Alto Douro, UTAD, Vila Real, Portugal;* [4]*Instituto Dom Luiz (IDL), Faculdade de Ciências, Universidade de Lisboa, Lisboa, Portugal;* [5]*DiSTeBA, Università del Salento, Lecce, Italy;* [6]*CMCC, Lecce, Italy;* [7]*Institute of Meteorology and Climate Research, Karlsruhe Institute of Technology, Karlsruhe, Germany;* [8]*Institute for Geophysics and Meteorology, University of Cologne, Germany;* [9]*Department FE12–Data Assimilation, Deutscher Wetterdienst, Germany*

(Manuscript received 4 October 2018; in final form 17 January 2017)

ABSTRACT

In this study, hemispheric climatologies of explosive cyclones (ECs) derived using a set of different cyclone detection and tracking methods (CDTMs) are analysed. The aim is to evaluate trends and regional characteristics of ECs discussing consensus and disagreement among methods. Areas of both hemispheres characterised by relatively frequent presence of ECs are considered, with particular emphasis on their extremes. Despite the considerable differences (up to 21-38% in the Northern/Southern Hemisphere) in the total number of ECs detected by the various CDTM, this study provides evidence of a good level of agreement among methods concerning spatial distribution of cyclogenesis, track density, their main characteristics (depth, speed, duration, deepening and normalised deepening rate), seasonality and trends. ECs are shown to be deeper, faster and long-lasting with respect to ordinary cyclones in both hemispheres. Southern Hemisphere ECs are typically more intense than those in Northern Hemisphere. On the other hand, ECs in the Northern Hemisphere are characterised by a stronger deepening rate over 6 h and 24 h than in the Southern Hemisphere. Atlantic ECs are usually faster, deeper and characterised by higher deepening and geostrophically adjusted deepening rate than in the Pacific. This is particularly true in the eastern part of the basin. In both basins, ECs in the western side are characterised by higher normalised deepening rates than in the eastern parts. In the Southern Hemisphere, ECs close to Southern Africa and Australia are usually faster, deeper and with higher deepening rates than those close to southern South America. On the other hand, ECs close to southern South America and Southern Africa are characterised by higher normalised deepening rates and duration with respect to ECs close to Australia.

Keywords: explosive cyclones, cyclone detection, tracking schemes, comparison, deepening rate, normalised deepening rate

1. Introduction

Cyclones are a key component in the mid-latitude atmosphere dynamics. They play a fundamental role in the hydrological cycle, in the meridional transport of energy, moisture and momentum (e.g. Peixoto and Oort, 1992). Cyclones are strongly linked with meteorological hazards, such as strong winds, marine storms, storm surges, intense precipitation, floods and landslides and, thus, with economic losses and fatalities (e.g. De Zolt et al., 2006; Nissen et al., 2010; Liberato et al., 2011; 2013; Pinto et al., 2013; Reale and Lionello, 2013; Liberato, 2014).

Explosive cyclones (or so-called meteorological "bombs", hereafter ECs) are characterised with respect to "ordinary" cyclones (or non-explosive cyclones, hereafter NECs) by a strong deepening rate (depending on latitude) in a relative short time range. Historically, ECs are identified through a "Normalised Central Pressure Deepening Rate" (NDR_c, Sanders and Gyakum, 1980) defined as:

*Corresponding author. e-mail: reale.marco82@gmail.com

Citation: Tellus A: 2019, **71**, 1611340, https://doi.org/10.1080/16000870.2019.1611340

$$(DR_{24h}/24h) * \sin(60^{\circ})/\sin(\varphi) \quad (1)$$

where DR_{24h} is the variation of central pressure over a period of 24 h, φ is the latitude of cyclone and 60° is the so-called "reference latitude". When NDR_c exceeds the unity, the system is deemed to be an EC (Sanders and Gyakum, 1980). In the Southern Hemisphere this definition has been challenged as it may lead to the identification of many artificial/spurious systems (Lim and Simmonds, 2002; Allen et al., 2010). In fact, according to (1) a system moving meridionally towards a lower pressure area experiences a strong deepening due to the variation of pressure field background that does not correspond to a real increase in the strength of the system itself. Therefore, it has been suggested to use either a "Normalised Reference Pressure Deepening Rate" (NDR_r) so that $DR_{24\,h}$ corresponds to the anomaly with respect to the climatology field, or to use an approach combining NDR_r/NDR_c metrics together (Lim and Simmonds, 2002; Allen et al., 2010).

ECs form in both hemispheres mainly during the cold season in regions with enhanced baroclinicity associated to strong horizontal temperature gradients (e.g. to the east of continental coastlines), large moisture availability and enhanced jet stream velocities (Roebber, 1984; Sanders, 1986; Gyakum et al., 1989; Chen et al., 1992; Stull, 2000; Chang et al., 2002; Allen et al., 2010; Seiler and Zwiers, 2016). Due to the rapid decrease of the central pressure, these systems are associated with extreme strong circulation and thus with extreme events like wind gusts, heavy rain potentially leading to floods, and extreme height waves (Sanders and Gyakum, 1980; Fink et al., 2009; Liberato et al., 2011).

Over the last 40 years, studies on ECs have been focused on deriving a climatology in Northern/Southern Hemisphere (hereafter NH/SH; e.g. Roebber, 1984; Lim and Simmonds, 2002; Allen et al., 2010; Seiler and Zwiers, 2016) or in specific regions (Sanders, 1986; Chen et al., 1992; Wang and Rogers, 2001; Trigo, 2006; Kuwano-Yoshida and Asuma, 2008; Kouroutzoglou et al., 2011), on associated physical processes and teleconnections (e.g. Fink et al., 2012; Gómara et al., 2014) or on specific case studies (e.g. Liberato et al., 2011; Ludwig et al., 2014). For example, Allen et al. (2010) have shown that ECs are distributed into several distinct regions, including two regions of maximum density in the NH corresponding to the Northwest Pacific and North Atlantic and three regions in the Southern Hemisphere in correspondence to East of Southern America, between 45E–90E, poleward of 40S and in an area corresponding to 100E–150W/45S-80S. Seiler and Zwiers (2016) have evaluated the ability of CMIP5 to reproduce ECs and shown that most of the models reproduce well their spatial distribution in comparison with the reanalyses in the NH, with two maxima along the Kuroshio and the Gulf Stream. Furthermore, Liberato et al. (2011) have analysed the case of the storm Klaus, which affected Europe (mainly France and Spain) on 23–24 January 2009 and was associated with heavy rain, snow over the Pyrenees, record breaking wind gusts (up to 55 ms^{-1}), high waves over the Bay of Biscay and Western Mediterranean (up to 15 m) and considerable societal impacts including fatalities. All these studies have applied cyclone detection and tracking methods (hereafter CTDMs; Neu et al., 2013; Lionello et al., 2016) to reanalyses or climate models data.

While the above-described climatological studies are valid assessments of the ECs activity in both hemispheres, they can be influenced by the choice and resolution of the reanalyses/GCMs used and by the choice of CDTM itself (Allen et al., 2010). For example, depending on how a cyclone is defined, a CDTM may use for the detection and tracking different atmospheric variables, such as mean sea level pressure (MSLP) or relative vorticity (Neu et al., 2013), leading to the identification of different position centres and intensification rates for the same storm.

The IMILAST (Intercomparison of MId LAtitude STorm Diagnostics, Neu et al., 2013; Ulbrich et al., 2013; Hewson and Neu, 2015; Rudeva et al., 2014; Lionello et al., 2016; Pinto et al., 2016; Grieger et al., 2018) project has provided evidence of the potentiality of a multi CDTM approach for identifying and describing the entire life cycle of cyclones. Neu et al. (2013) have shown that all CDTMs approaches applied to ERA-interim dataset produce comparable climatologies of cyclones in the NH/SH, with a general high agreement among different CDTMs for deep cyclones and for the frequency, life cycle, inter-annual variability and trends of these systems. Based on selected case studies, Neu et al. (2013) showed that the level of agreement among CDTMs in describing the cyclone life cycle is high during the intense phase of the storm, low during its previous development and lysis. On the other hand, Ulbrich et al. (2013) have shown that despite different numbers of cyclones identified applying different CDTMs to ECHAM5/OM1 model simulation, the climate change signal is similar among all the CDTMs. Hewson and Neu (2015) have analysed the structure and characteristics of windstorms affecting Northern Atlantic and Europe identifying three causal classes of these systems. Rudeva et al. (2014) have analysed the sensitivity of cyclone climatology to the filtering over orography exceeding 1500 m, time of detection and representation of fast moving cyclones, providing evidence that filtering and late identification of cyclones reduces significantly the number of cyclones, while the splitting of trajectories has negligible effect on cyclone

distribution as well as on the average deepening rate. Lionello et al. (2016) have discussed the consensus among different CDTMs on the climatology of cyclones in the Mediterranean region, with a spread among methods mainly due to how each CDTM deals with slow and weak cyclones. Pinto et al. (2016) have shown that multi CDTMs approach qualitatively identifies cyclone clusters affecting the Euro-Atlantic Region in December–January–February and, in particular, that under dispersion and over dispersion of extratropical cyclones over the North Atlantic and Western Europe are features generally robust with respect to the choice of CDTM. Finally Grieger et al. (2018) analysed extratropical cyclone activity around the Antarctica showing that, despite a different number of tracks identified by each CDTM, the multi CDTMs pointed out the existence of robust trends in the area for these systems and that the level of agreement is high among the methods when the comparison is limited to stronger systems. All the previous works, thus, have pointed out that one of important source of spreading among different CDTMs rely on how these different approaches deal with slow/fast and weak/deep cyclones and a multi CDTMs approach can provide, indeed, a more robust description of cyclone activity in both hemispheres.

In the present manuscript, we focus on the characteristics of ECs from the multi-methodology CDTMs perspective. The main purposes of this work are as follows:

- to extract separated datasets of ECs and NECs for both hemispheres based on the original IMILAST dataset of cyclone tracks (Neu et al., 2013)
- to derive a comprehensive climatology of ECs in both hemispheres and assess their main characteristics with respect to NECs
- to use this climatology to compare characteristics of ECs among target regions in both hemispheres with particular emphasis on extremes, intensity and trends, assessing the statistical significance of the differences observed.

The work is organised as follows. Section 2 provides a description of the procedure for the identification of ECs, the features of the new ECs/NECs datasets and the statistical tools used in this work. Section 3 analyses the climatology of ECs in both NH/SH with a comparison of their features with respect to NECs and among themselves in different areas of both hemispheres. Finally, Section 4 includes the discussions of the results, conclusions and future developments of the work.

2. Data and methods

In this study, we consider ECs originated polewards beyond the 25° parallel in both hemispheres. The analysis of ECs activity and the relatively comparison with NECs is based on eight different CDTM (Table 1) applied to the Mean Sea Level Pressure (MSLP) fields of the 6-hourly ERA-Interim 1979–2008 at 1.5° resolution. For a full description of each CDTM, the reader is referred to Neu et al. (2013) and references in Table 1. Each CDTM provides a list of cyclones with a lifetime longer than 24 h, their position as a function of time and different variables describing their intensity (like MSLP, Laplacian, Geopotential Height, Neu et al., 2013). These CDTMs differ among them in employing different metrics for the detection and tracking of cyclones (such as minimum MSLP, Relative Vorticity, intensity of wind, maximum of Laplacian of SLP, maximum gradient of SLP) or different thresholds for removing/merging artificial/weak systems (Neu et al., 2013). Among the list of methods that contributed to the IMILAST dataset (Neu et al., 2013), we have chosen the eight tracking methods (Table 1) based on MSLP.

Table 1. List of cyclone detection and tracking methods used in this study with code number in the IMILAST dataset and main bibliographic reference for the description of each method.

Method	References
M02	Murray and Simmonds, 1991; Pinto et al., 2005
M06	Hewson, 1997; Hewson and Titley, 2010
M08	Trigo, 2006
M09	Serreze, 1995; Wang et al., 2006
M10	Murray and Simmonds, 1991; Simmonds et al., 2008
M16	Lionello et al., 2002; Reale and Lionello, 2013
M20	Wernli and Schwierz, 2006
M22	Bardin and Polonsky, 2005; Akperov et al., 2007

Cyclones for each of the methods have been then divided in ECs and NECs and two separate datasets have been built covering the period January 1979–December 2008. The variables used to describe both classes of cyclones are: position (in longitude and latitude), SLP value of the central minimum (hPa), deepening rate (DR_{6h}, hPa/6h), geostrophically adjusted deepening rate (ADR_{6h}, hPa/6h), normalised central deepening rate (equation 1, NDR_c in hPa/24h), adjusted normalised central deepening rate ($ADNDR_c$, in hPa/24h), speed (in km/h), distance covered in 6 h (in km) and two flags (0 or 1) to mark when the cyclone becomes EC and reaches its maximum ADR_{6h}. These variables are defined as follows:

- DR_{6h}: the variation of pressure in a cyclone in two consecutive timesteps
- ADR_{6h} (Trigo, 2006): $(DR_{6h})*\sin(60°)/\sin(\varphi)$ where φ is the latitude of cyclone and 60° is the so-called reference latitude
- $ADNDR_c$: $(DR_{24h}/24h)*\sin(60°)/\sin(\varphi_{av})$ where φ_{av} is the latitude of the mean position of cyclone in 24h and 60° is again the reference latitude

Table 2. Number of NECs/ECs detected in each list before (first and third columns) and after (second and fourth columns) applying the filter on the maximum velocity.

	Northern hemisphere		Southern hemisphere	
Method	All	Max speed< =150 km/h	All	Max speed< =150 km/h
M02	65712/5182	62973/4781	52318/9518	49747/8581
M06	79015/3284	78969/3282	85904/7554	85836/7553
M08	46538/2968	46535/2968	40081/4461	39998/4461
M09	95293/3068	93024/2960	51071/4207	49942/4035
M10	39322/3042	39151/2994	45209/6777	44969/6609
M16	57938/3747	50669/2753	44772/5082	40336/3710
M20	61139/2520	60774/2468	38304/3117	38071/3068
M22	63201/3246	63152/3244	40148/4325	39932/4320

In the computation of NDR_c and $ADNDR_c$, following the IMILAST protocol (Neu et al., 2013), we considered 24 h as a period of five consecutive time steps.

ECs are defined as all the systems which fulfil the criteria of equation (1) based on the NDR_c (Sanders and Gyakum, 1980) while the category NECs includes all the systems which does not fulfil the criteria based on equation (1) and has a maximum ADR_{6h}/NDR_c lower than zero (this in order to filter away systems identified by each CDTM with no negative observed deepening rates along their life cycle). Recently, the criterion of equation (1) has been criticised and other criteria have been suggested (Allen et al., 2010). However we have kept the original formulation, as the main purpose of this work is not to compare the sensitivity of the climatology of ECs with respect to different detection criteria, but to derive a general climatology using a multi tracking approach.

Following the multi tracking approach introduced in previous works (Neu et al., 2013; Ulbrich et al., 2013; Hewson and Neu, 2015; Rudeva et al., 2014; Flaounas et al., 2016; Lionello et al., 2016; Pinto et al., 2016) we explore the consensus in term of trends for the ECs computing a multi-method mean (MCDTM, Neu et al., 2013; Lionello et al, 2016). To show a possible common behaviour among the time series in both hemispheres a normalised index EC_{index} has been computed for each *i*-method, defined as

$$EC_{index}(i,t) = \left(EC(i,t) - EC_{average}(i)\right)/stdEC(i) \qquad (2)$$

where $EC(i,t)$ is the number of ECs in the *i*-method at the time *t*, $EC_{average}(i)$ the average of the timeseries, stdEC(i) is its standard deviation. The Mann–Kendall test (MK) has been adopted for assessing the significance of trends in the historical time series. Additional statistical tools are considered and described in the regional analysis (Section 3.3).

Finally, boxplots are used to compare ECs and NECs in order to determine the most frequent minimum value of SLP (hereafter $MSLP_{min}$, meant for the whole duration of the cyclone) and the most frequent maximum value of DR_{6h}, ADR_{6h}, NDR_c, speed (hereafter DR_{max}, ADR_{max}, NDR_{cmax}, $speed_{max}$) and duration at hemispheric scale. Particular emphasis has been given to extremes in some selected areas of both Hemispheres.

3. Results

3.1. ECs climatologies

Table 2 shows the number of NECs/ECs detected in each hemisphere and those systems retained after discarding systems with a maximum value of speed along their life cycle, greater than 150 km/h. This filter is required because some CDTMs (e.g. Rudeva et al., 2014) tend to merge two close cyclone tracks in one track giving rise to unrealistic propagation speed (in some cases also greater than 300 km/h) and strong deepening rate, mimicking an explosive development.

Quantitative differences in the numbers of NECs/ECs among CDTMs are relatively large for both hemispheres. In the NH the average number of ECs(NECs) per year is equal 110 ± 26 (2113 ± 548) for the full analysed period, with a spread among the methods measured by the coefficient of variation[1] approximately equal to 24% (26%). In the SH, the average number of ECs(NECs) is 187 ± 71 (1657 ± 516), with a spread among the methods approximately equal to 38% (31%). All methods show that ECs are much less frequent than NECs, with the average ratio ECs/NECs in NH (SH) equal to 5% (11%).

The relative importance of ECs versus NECs appears to remain substantially unaltered if all systems with maximum speed observed greater 150 km/h are discarded. CDTMs are sensitive at a different extent to this threshold depending on hemispheres as well. Comparing all methods for the NH, the average number of ECs(NECs) per year decreases to 104 ± 22 (2065 ± 545), with a spread in both categories among the methods approximately equal to 21% (26%). In the SH, the average number of

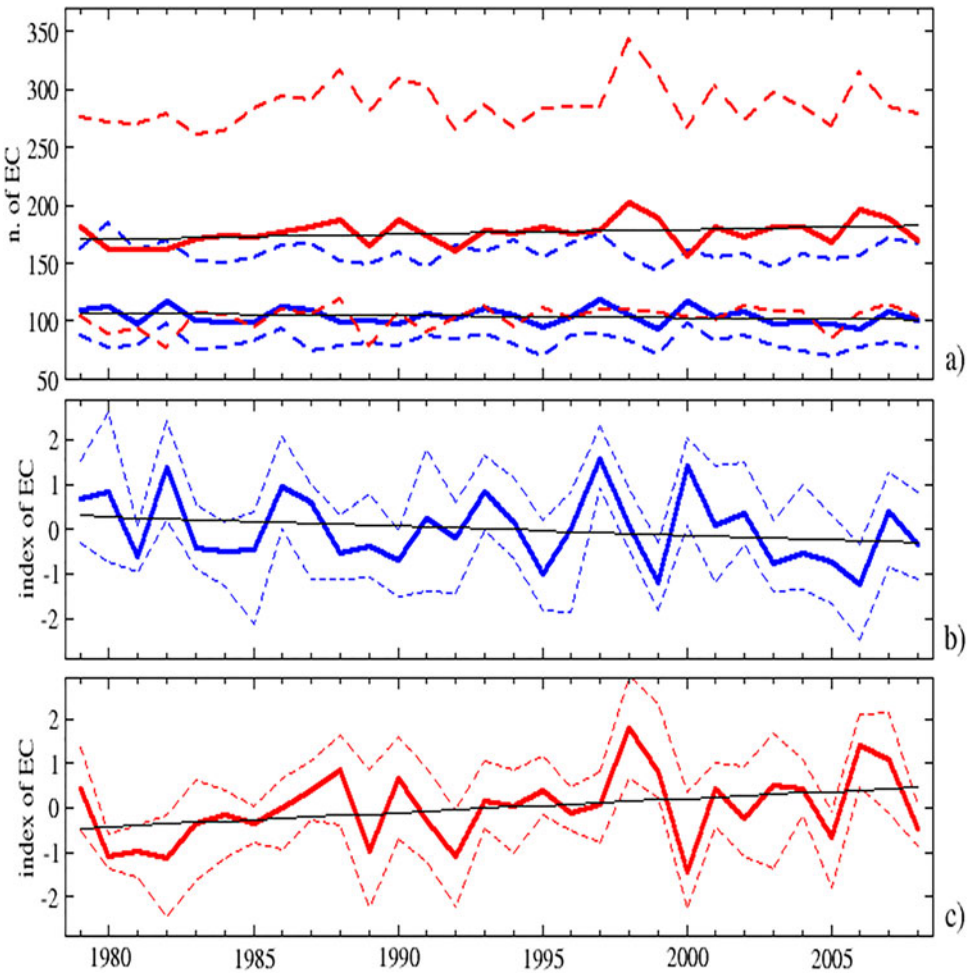

Fig. 1. (a) Time series of interannual variability of ECs in NH (blue) and SH (red). Thick line shows the MCDTM, respectively, for NH (blue) and SH (red). Dashed lines mark the spread of all the data in NH (blue) and SH (red). EC_{index} is shown in NH (b, blue) and SH (c, red). Thick line shows the MCDTM EC_{index}, respectively, for NH (blue) and SH (red). Dashed lines mark the spread of all the data in NH (blue) and SH (red). Black lines show the tendency line computed trough a linear fit.

ECs (NEC) decreases to 176 ± 67 (1620 ± 524) with a spread among the methods approximately equal to 38% (32%). It appears that the uncertainties raising from very fast propagating cyclones affect mainly ECs in the NH and it is probably linked to the larger area with orography higher than 1500 m in the NH, where this error has been observed (Rudeva et al., 2014). For the rest of the paper the analysis will include only ECs and NECs with maximum propagation speed lower than 150 km/h. The number of ECs detected in NH (SH) tends to be higher (is in good agreement) with respect to Allen et al. (2010) (80 ECs in the NH and 171 ECs per year in SH) and higher with respect to Lim, and Simmonds (2002) (26.4 ECs in the SH and 45.9 in the NH). However, these numbers are not directly comparable with our results as in Allen et al. (2010) a single CDTM was employed while in Lim and Simmonds (2002) the detection of ECs has been carried out using NDR_r approach instead of our classical approach.

3.2. Temporal and spatial variability of ECs

Figure 1(a) shows the historical MCDTM annual time series of ECs in blue (red) for the NH (SH) together with the spread of all data (dashed lines) for each hemisphere.

The NH (SH) MCDTM is characterised by a slight negative (positive) trend estimated by least square resulting equal to –0.2 (0.4) ECs $year^{-1}$. Only the tendency observed in the SH results significant at 95% level according to MK ($p < 0.05$) and is comparable with the value found by Lim and Simmonds (2002) who estimate a value of 0.56 ECs $year^{-1}$ (also in this case statistically

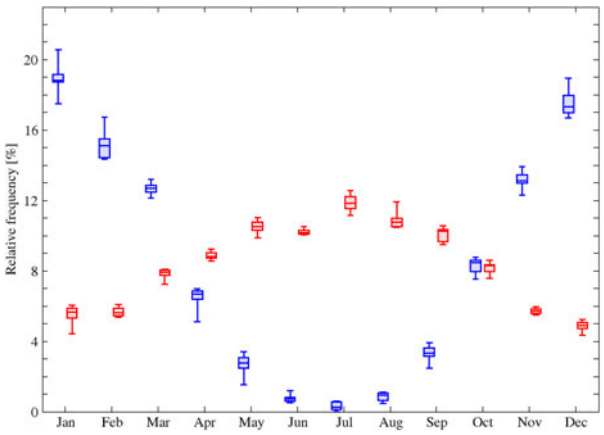

Fig. 2. Inter-monthly relative frequency (in %) of ECs in NH (blue) and SH (red). The upper and lower limits of the boxes correspond to 25th and 75th percentiles, the whiskers represents the min/max values, and – represents the median among the methods in each month.

significant). The positive tendencies observed in the NH by Lim and Simmonds (2002) and Allen et al. (2010) were not statistically significant. Figure 1(b,c) shows the time series of the corresponding EC_{index} described in equation (2) for both hemispheres. The spread among the methods dramatically reduces and again the MCDTM shows in NH (SH) a slight negative (positive) linear trend equal to –0.02 (0.03).

Figure 2 shows the mean annual cycle of ECs in the NH and SH. In the NH, ECs frequency is relatively high in winter (ONDJFM), and lower in summer (JJA). In particular, the period ONDJFM accounts for more than 80% of ECs detected in NH. In the SH, the seasonal variability is relative low with respect to NH (Lim and Simmonds, 2002; Allen et al., 2010) with a peak during the cold austral season. In the SH, the period AMJJASO accounts for more than 70% of the total number of ECs detected. January (July) is the month in the NH (SH) where ECs activity has its own peak with a frequency of 19% (12%). The lowest value in NH is observed in JJA (<1%), while in the SH this minimum is observed in December (5%).

Figure 3(a,b) and Figure 4(a,d) show, respectively, the MCDTM density (measured as relative frequency map, %, of ECs counted in each cell of 1.5°*1.5°) of tracks (Fig. 3a,b), cyclogenesis (Fig. 4a,b) and explosive deepening (Fig. 4c,d) of ECs in NH (first column in both figures) and SH (second column). The fraction of cell filled represents the level of agreement among methods which is measured by the normalised standard deviation (std_{MCDTM}/MCDTM; Lionello et al., 2016). A decreasing fraction of cell filled corresponds to a decreasing agreement among methods. In the NH (Fig. 3a) ECs move mainly along the Atlantic/Pacific storm tracks close to the eastern North American (Roebber, 1984; Lim and Simmonds, 2002; Allen et al., 2010) and Japanese coastlines (Lim and Simmonds, 2002; Allen et al., 2010; Kuwano-Yoshida and Enomoto, 2013). In the Pacific the ECs tracks show a more zonal orientation than in the Atlantic, where they exhibit a NE–SW orientation, as already pointed out in previous works (e.g. Lim and Simmonds, 2002). In the SH (Fig. 3b) the MCDTM shows a large maximum off the east coast of southern South America (Lim and Simmonds, 2002; Hoskins and Hodges, 2005; Allen et al., 2010) forming a sort of spiral all around and ending on the Antarctica. Secondary signals are located at the lee of Rocky/Himalaya chains in NH and of Andes in SH and in the Mediterranean region associated here with Mediterranean storm track (Flaounas et al., 2016; Lionello et al., 2016). The MCDTM for cyclogenesis (Fig. 4a) shows that in NH, ECs genesis takes place in the same areas identified for NECs (e.g. Neu et al., 2013): the eastern North America and Japanese coastlines (Roebber, 1984; Allen et al., 2010; Neu et al., 2013), the Central Pacific, the lee of the Rocky Mountains (Roebber, 1984). Due to the low level of agreement among the methods a weak signal related to the cyclogenesis can be observed in the Western Mediterranean region (Lionello et al., 2016). In the SH the maximum of cyclogenesis (Fig. 4b) is observed off the southern South America coastlines and the oceanic area surrounding the Antarctica (Lim and Simmonds, 2002; Allen et al., 2010; Neu et al., 2013). The MCDTM explosive deepening (Fig. 4c,d) occurs prevalently over open ocean areas with enhanced baroclinicity/strong horizontal SST gradients, such as the area of Gulf stream, Kuroshio and, in the SH, along the Antarctic Circumpolar current (e.g. Roebber, 1984; Lim and Simmonds, 2002; Allen et al., 2010). Maxima of explosive deepening are present in the NH (SH) at the lee of Rocky and Himalaya (Andes) Mountains. Again in the Mediterranean region it is possible to observe some explosive deepening areas like the Gulf of Genoa and Ionian Sea which have been already identified in previous studies (e.g. Kouroutzoglou et al, 2011). In the NH (SH) the areas of maximum frequency of explosive deepening (Fig. 4c,d) are shifted eastwards (polewards) with respect to those where cyclogenesis occurs (Fig. 4a,b). The agreement regarding the ECs tracks (cyclogenesis) is maximum along the Atlantic/Pacific storm tracks (close to the eastern North American/Japanese Coastlines) and around the Antarctica (off the southern South American coastlines and around Antarctica coastlines) and it decreases over the continental areas (e.g. Lim and Simmonds, 2002; Allen et al, 2010; Neu et al., 2013). The agreement among the methods on the frequency of ECs explosive deepening is high (low) over the oceanic areas (the continental

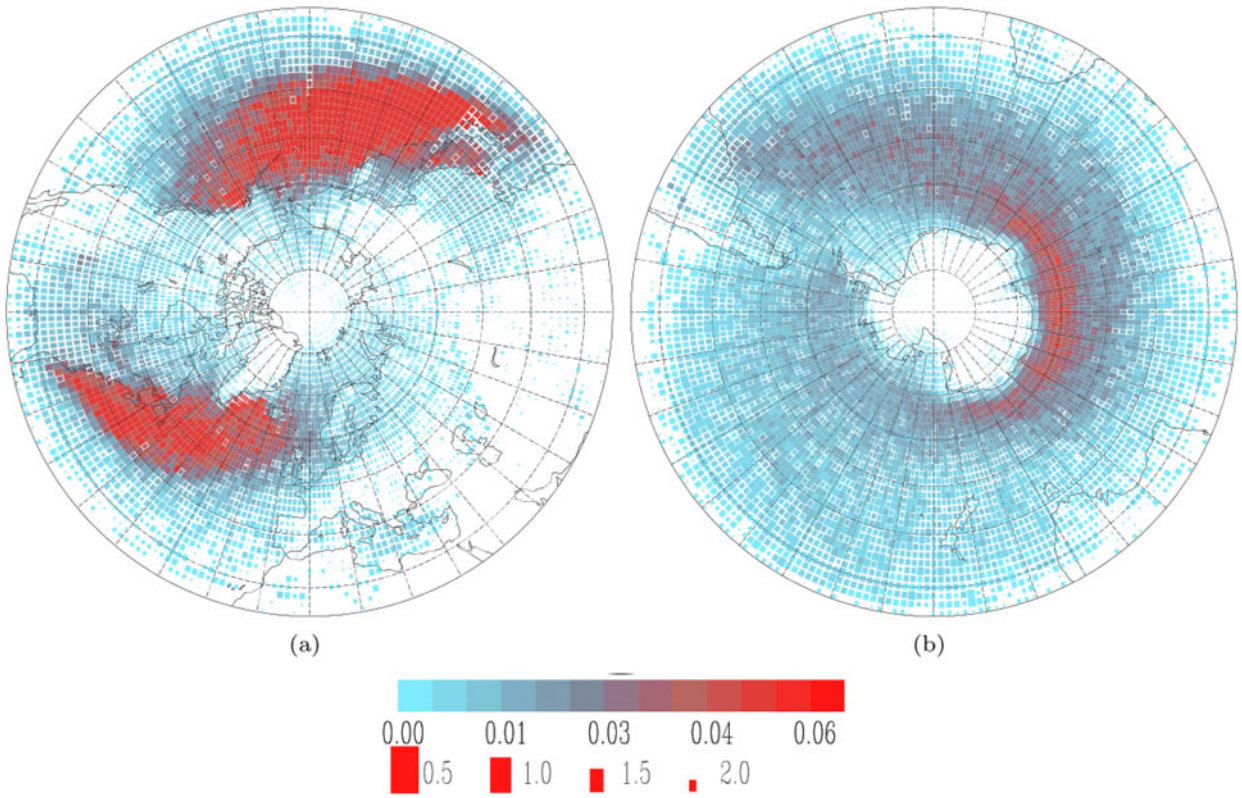

Fig. 3. Track (a,b) density of ECs according to the MCDTM in NH (first column) and SH (second column). Colors represent the probability (%) that a cyclone track crosses each 1.5 x 1.5 cell of the domain in the 6-hourly field (values according to the label bar below the panels). The filled fraction of each cell corresponds to the level of agreement (given by the normalised standard deviation) among methods as annotated below the panels.

areas) in both Hemispheres, confirming that explosive deepening is mainly an oceanic process. Despite different approaches among the methods in identifying and tracking cyclones, it is possible, thus, to identify robust signal in the MCDTM concerning tracks, cyclogenesis and deepening areas for ECs.

3.3. Comparison between ECs and NECs in both hemispheres

Figure 5(a,b) compares the relative frequency of NECs and ECs in function of the $MSLP_{min}$ in the NH (a) and SH (b) by using boxplots to show the variability within a certain core pressure range. In the NH about the 57% (66%) of ECs(NECs) has a minimum value along its life cycle of sea level pressure falling between 960 and 980 hPa (990 and 1010 hPa). In the SH (b) about 52% (64%) of ECs(NECs) has a minimum value along its life cycle of sea level pressure falling between 940 and 960 hPa (960 and 1010 hPa). Figure 5(c,d) compares the relative frequency of NECs and ECs in function of $speed_{max}$ along its life cycle. In both Hemispheres about 78%(64%) of ECs(NECs) has a maximum speed value falling between 60 and 120 km/h (40 and 100 km/h). Finally over 54% of NECs in both Hemispheres (Fig. 5e,f) has a life cycle lasting until 72 h, while about 51%(54%) of ECs in the NH (SH) last at least 72–144 h. Therefore, ECs are substantially deeper than NECs; still they tend to be faster and to have a longer duration than NECs.

Comparing the two hemispheres, ECs in the SH tend to last longer and to be deeper than ECs in the NH. This last result appears in contrast with previous works (e.g. Lim and Simmonds, 2002), who have found that NH ECs are usually deeper than SH ECs. However, Lim and Simmonds (2002) include in their definition of depth not only the simple $MSLP_{min}$ but the effect of background SLP field that is not included in our analysis. No differences are apparent between ECs in the two hemispheres concerning $speed_{max}$. This may be unexpected, as Lim and Simmonds (2002) provided evidence that SH ECs are usually faster than NH ECs. According to Lim and Simmonds (2002), the difference in mean ECs speed

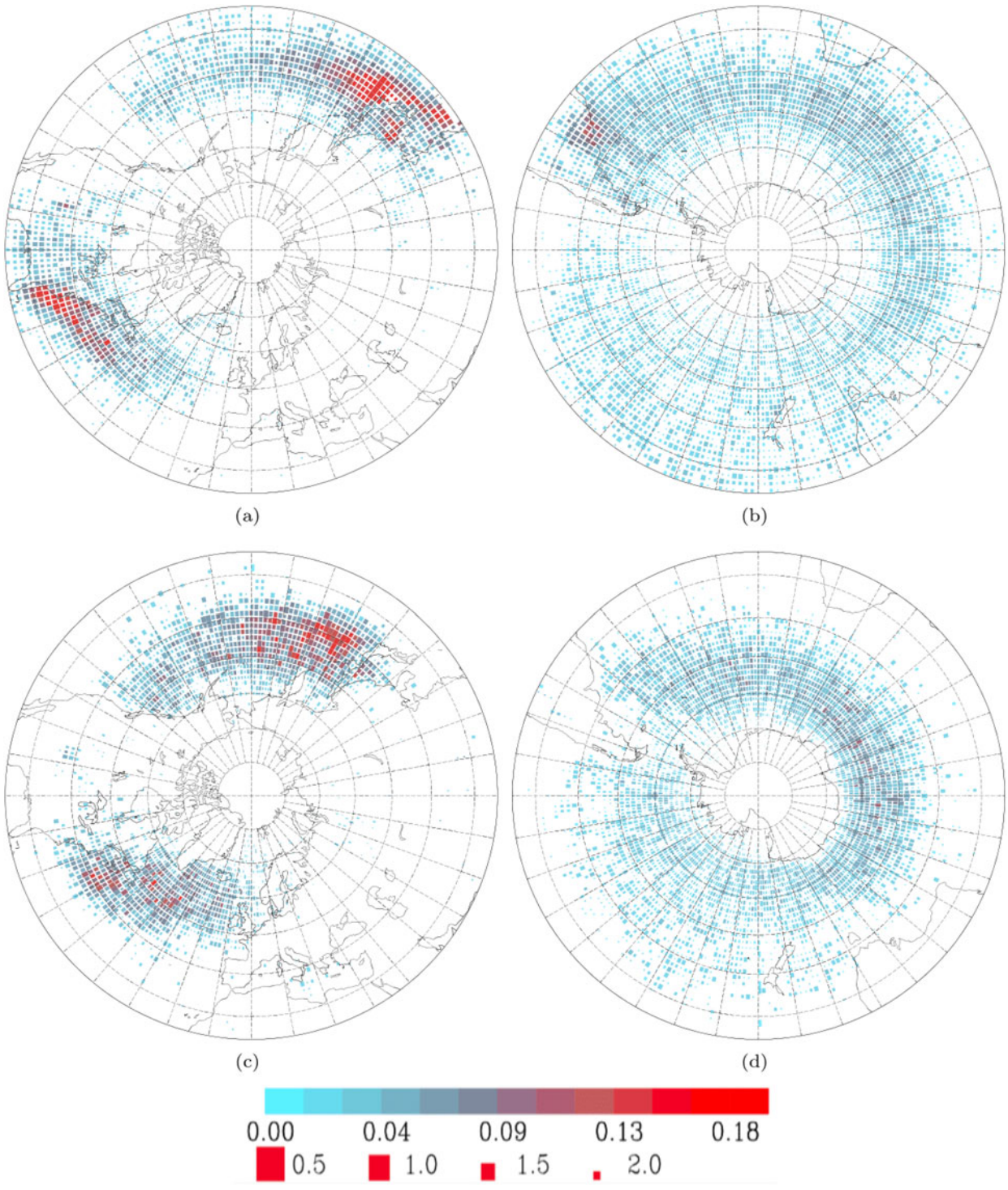

Fig. 4. Same as Fig. 3 but for cyclogenesis (a,b) and explosive deepening (c,d).

between the two hemispheres is approximately 1.1 m/s (~4 km/h). Given that the width of bins used here is 20 km/h (cf Fig. 5c,d), they may not be able to identify small differences in ECs $\text{speed}_{\text{max}}$ between the two hemispheres.

Figure 6(a–f) compares the relative frequency of ECs and NECs in function of their DR_{max}, ADR_{max} and NDR_{cmax}. Obviously, there are substantial differences between ECs and NECs. About 78% (89%) of ECs(NECs) in NH (Fig. 6a,b) has a maximum DR

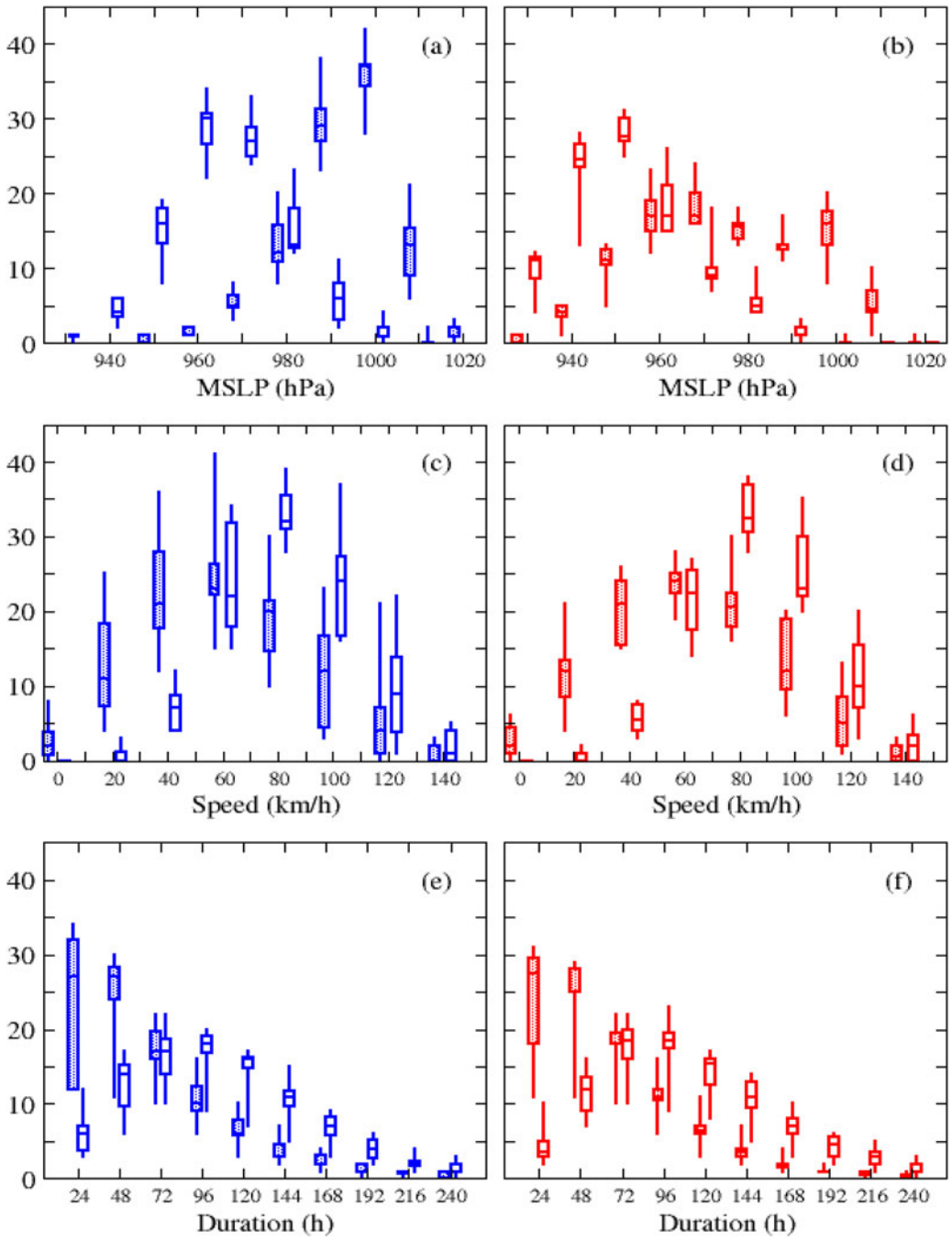

Fig. 5. Relative frequency (%) of NECs (full box) and ECs (empty box) in NH (blue) and SH (red) as function of: (a,b) their lifetime $MSLP_{min}$ considering 10 hPa wide bins and covering the range from 930 to 1020 hPa, (c,d) $speed_{max}$ (in km h^{-1}) considering 20 km/h wide bins and covering the range 0–140 km/h, (e,f) duration (in h) considering 24 h wide bins and covering the range 0–240 h illustrated by box plots: the NH (first column) and SH (second column). The upper and lower limits of the boxes correspond to 25th and 75th percentiles, the whiskers represents the min/max values, – represents the median among the methods in each month.

falling between –12 and –6 hPa/6h (–6 and 0 hPa/6h). In SH about 85%(86%) of ECs (NECs) have a maximum DR falling –12 and –6 hPa/6h (–6 and 0 hPa/6h). About 70% (78%) of ECs (NECs) in NH (Fig. 6c,d) has a maximum ADR falling between –12 and –6 hPa/6h (–6 and 0 hPa/6h). In the SH about 82%(79%) of ECs (NECs) has a maximum ADR falling –12 and –6 hPa/6h (–6 and 0 hPa/6h) (Fig. 6c,d). Finally about 59%(64%) of ECs (NECs) in NH (Fig. 6e,f) has a maximum NDR_c falling between –32 and –24 hPa/24 h (–4

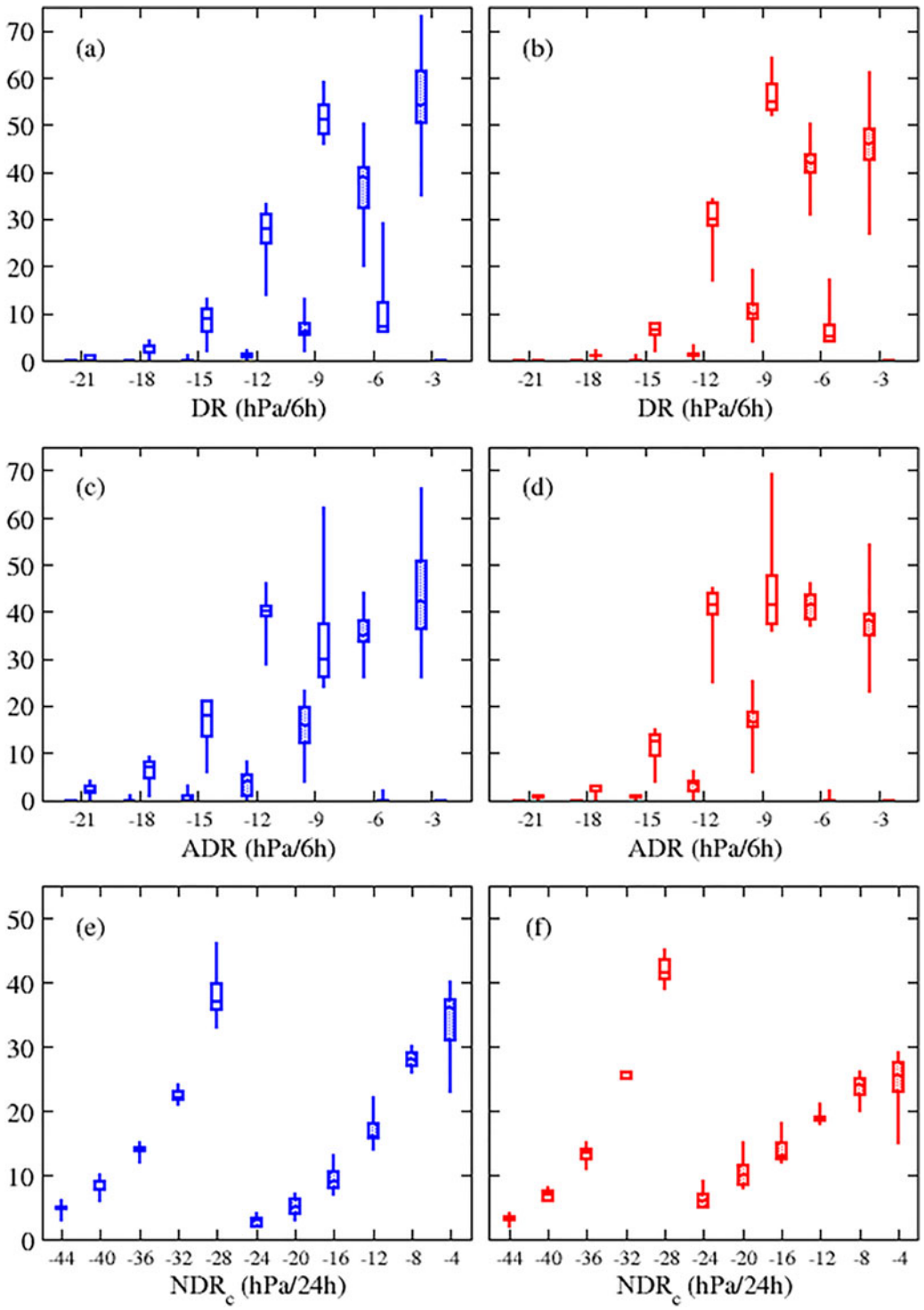

Fig. 6. Same as Fig. 5 but (a,b) DR_{max} (in hPa/6h) considering 3 hPa wide bins and covering the range from –21 hPa/6h to 0 hPa/6h, (c,d) ADR_{max} (in hPa/6h) considering 3 hPa wide bins and covering the range –21 hPa/6h to 0 hPa/6 h, (e,f) NDR_{cmax} (in hPa/24h) considering 4 hPa wide bins and covering the range from –44hPa/hPa to 0 hPa/24 h.

and 0 hPa/24 h). In SH about 56%(49%) of ECs(NECs) have a maximum NDR_c falling –32 and –24 hPa/24 h (–4 and 0 hPa/24 h).

The statistical distribution of ECs in NH with respect to their deepening rate metrics (DR_{max}, ADR_{max}, NDR_{cmax}) is slightly shifted towards greater values than

Table 3. Median of 25th, 50th, 75th and 90th related to the $MSLP_{min}$, DR_{max}, ADR_{max}, NDR_{cmax}, $speed_{max}$ and DURATION of ECs in NH (black) and SH (red).

Metric	25th	50th	75th	90th
$MSLP_{min}$ (in hPa)	988.42/974.87	978.42/963.40	969.3/953.20	960.9/944.34
DR_{max} (hPa/6h)	–7.6/–7.76	–8.91/–8.91	–10.63/–10.43	–12.83/–12.17
ADR_{max} (hPa/6h)	–9.17/–8.72	–10.76/–9.93	–13.12/–11.58	–15.81/–13.55
NDR_{cmax} (hPa/24h)	–26.37/–26.01	–29.64/–28.70	–35.14/–32.86	–41.70/–37.80
$speed_{max}$ (km/h)	76.38/76.51	92.63/91.58	107.17/107.2	121.11/122.90
DURATION (h)	72/78	108/108	144/147	186/192

in SH, suggesting in general larger deepening rates. This is in agreement with previous studies (Lim and Simmonds, 2002; Allen et al., 2010), which have shown that extreme values of NDR_c are more frequent in the NH, as it is characterised by pronounced baroclinic environment with respect to the SH.

Finally, Table 3 shows the 25p, 50p, 75p, 90p thresholds for the NH (black) and SH (red) for the metrics describing the intensity and the dynamics of ECs. Each value shown is the median of each set of percentile thresholds (25p, 50p and so on) built with all the CDTMs. For example, 25th value shown in Table 3 has been computed taking the median of all 25^{th} thresholds computed considering all the CDTMs. Table 3 confirms the differences observed in Figs. 5 and 6 between NH and SH. ECs in the SH tends to be deeper and long lasting with respect to ECs in NH (Sanders, 1986; Lim and Simmonds, 2002) while ECs in the NH are characterised by stronger deepening rate on both 6 h and 24 h time intervals (Sanders, 1986; Lim and Simmonds, 2002).

3.4. Regional comparison of ECs

Here we investigate differences in the ECs characteristics among areas, mainly over the ocean (where the dispersion among CDTMs is lower, Figs. 3 and 4), in the same hemisphere, due to local factors such as baroclinicity, air-sea interactions and SST horizontal gradients. With this goal, a specific regional analysis of ECs has been carried out.

We consider three categories of EC for each considered metric ($MSLP_{min}$, $speed_{max}$, duration, DR_{max}, ADR_{max}, NDR_{cmax}) based on three of the five thresholds of percentile introduced in Table 3. Being "X" (e.g. $speed_{max}$) the considered metric, we define X[0p,50p] the category including all ECs in a specific area with a maximum value of X lower than 50p (as reported in Table 3). X[50p,75p] is the category including ECs in a specific area with a maximum value of X in the range from the 50p to the 75p while X[75p,100p] is the category including those systems in the same area with a maximum value of X greater than 75p.

The analysis is carried out for selected areas according to the following criteria: (i) the methods spatially agree best according to normalised standard deviation (and, thus, the statistical dispersion among the methods is low, Figs. 3 and 4), (ii) the impacts of related extreme events can be high (due to large human population potentially affected), (iii) the cyclone activity is high (in terms of cyclogenesis, density of tracks, deepening processes (Allen et al., 2010; Neu et al., 2013). Only ECs becoming explosive inside the selected areas have been taken into account for the statistical analysis, independently from their cyclogenesis area.

3.4.1. Northern hemisphere. Figure 7(a) shows four areas selected in the NH: WPAC (West Pacific, blue), EPAC (East Pacific, red), WATL (West Atlantic, green), EATL (East Atlantic, fuchsia). The size of the four areas is quite comparable in each basin (71581 km^2 for WATL, 71702 km^2 for EATL, 104815 km^2 for WPAC and 97145 km^2 for EPAC).

A preliminary analysis has been done to exclude the sensitivity of our results to small shifts in the position of the areas themselves. For each area we repeated the analysis done in Section 3.3. We checked the variation of the results when each area is shifted from one up to three degrees in northward/southward/eastward/westward direction (not shown). No significant effect of such small shifts has been found, except when they increase the fraction of land included, because, being the agreement among methods over land lower than over sea, the statistical dispersion among the methods increases.

In the NH this analysis considered an extended winter season ONDJFM, as this period accounts for more than 80% of ECs in the NH (see Section 3.2) so that it can be considered quite representative of ECs activity. In the period ONDJFM 1978-2008 an average number per year of 35 ± 6 ECs has been found in WPAC, 21 ± 5 in EPAC, 19 ± 5 in WATL and 13 ± 3 in EATL. Thus, the highest number of ECs in each ocean basin is observed in their western part (Roebber, 1984; Allen et al., 2010; Neu et al., 2013) confirming that western continental coastlines are the areas where ECs are more frequent. In all these areas, MCDTM trends are not statistically

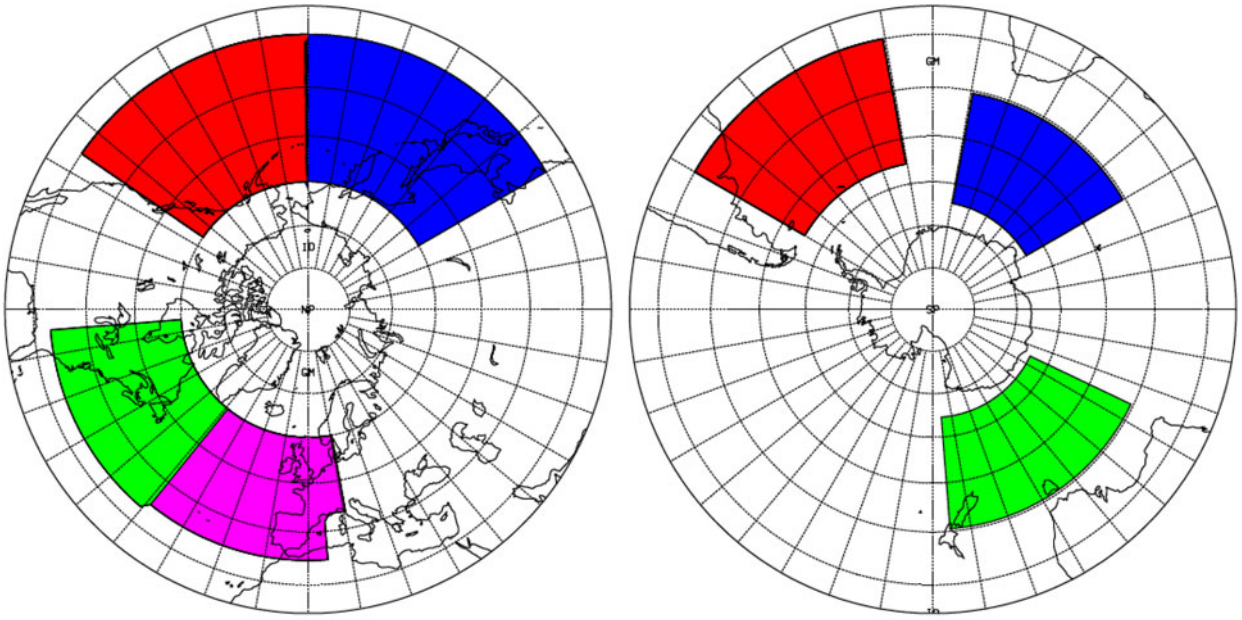

Fig. 7. Areas selected for the regional analysis in NH (a): WPAC (blue), EPAC (red), WATL (green), EATL (fuchsia). SH (b): SAME (red), SAFR (blue), AUST (green).

significant. Finally the frequencies observed of ECs in each category computed for each area and for each metric have been tested[2] to check if the differences observed in the values for the same category (e.g. $MSLP_{min}$[75p,100p]) among areas in the same basin (as WATL and EATL) or opposite basins (as WATL and WPAC) were statistically significant or not. Only results statistically significant (at 90% of confidence level) will be reported and discussed in the next lines.

Figure 8a,b shows the relative of frequency of ECs (with respect to the population of ECs in each area) in WPAC, EPAC, WATL, EATL in each of the three categories previously introduced with X corresponding to $speed_{max}$ (a) and duration (b). Faster systems ($speed_{max}$[75p,100p]) are more frequent in Atlantic with respect to the Pacific. In fact about 31% of ECs detected in the EATL and 26% of ECs detected in WATL belong to $speed_{max}$[75p,100p] with respect to 22% of ECs observed in WPAC and 25% of ECs observed in EPAC. On the other hand, slower systems ($speed_{max}$[0p,50p]) are more common in the Pacific with a 57% (53%) of ECs detected in the WPAC(EPAC). In the Atlantic region the same systems represent the 51% of ECs found in WATL and 42% of ECs found in the EATL. The differences in the frequency values observed for both categories in the case of WATL/EATL, WATL/WPAC, EATL/EPAC are all statistically significant. For the couple WPAC/EPAC the only statistically significant difference has been observed for the categories $speed_{max}$[0p,50p].

Long-lasting systems (Fig. 8b, DURATION[75p,100p]) are prevalent in the western Pacific (WPAC 28%) and EATL (27%) while this category shows a minimum of frequency equal to 18% in WATL and a frequency of 26% in the EPAC. Short lasting systems (DURATION[0p,50p]) are prevalent in latter areas WATL (60%) and EPAC (53%) while they show a minimum of frequency in the WPAC and EATL (both 48%). The differences observed in the frequency values in both categories are statistically significant comparing the Atlantic areas (WATL/EATL) and the western part (WATL/WPAC) of both basin. In the eastern part of the basins (EATL/EPAC) and in the Pacific (WPAC/EPAC) the only statistical significant difference has been observed for the category DURATION[0p,50p]. Still in the Pacific (WPAC/EPAC) the intermediate category (DURATION[50p,75p]) shows another statistically significant difference in the frequency values observed which are, respectively, equal to 25% (WPAC) and 21% (EPAC).

The differences observed in speed and duration of ECs are likely to be associated with the enhanced baroclinicity and strong westerly flow (e.g. Lim and Simmonds, 2002) which characterise the Atlantic region (strong land-sea contrasts which occurs over shorter distance in the area; e.g. Raible, 2007) which allows the extremes related to speed to be more frequent in the Atlantic (mainly in its eastern part) with respect to the Pacific. The major frequency of extremes concerning the duration in Eastern

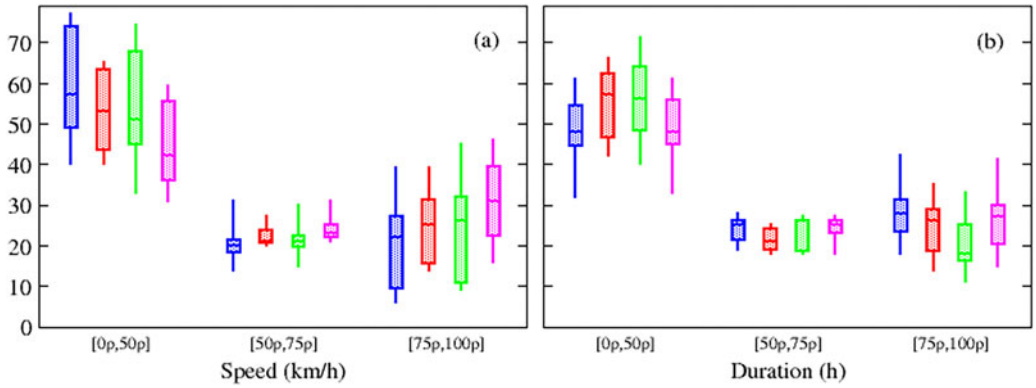

Fig. 8. Relative frequency (%) of X[0p,50p], X[50p,75p], X[75p,100p] with X corresponding to $speed_{max}$ (a) and duration (b) in WPAC (blue), EPAC (red), WATL (green) and EATL (fuchsia) as function of $speed_{max}$ (a) and duration (b) value falling in the percentile interval based on a hemispheric pdf for ECs. The upper and lower limits of the boxes correspond to 25th and 75th percentiles, the whiskers represents the min/max values, and – represents the median among the methods in each month.

Atlantic is probably a consequence of high frequency of cyclones formed on the western Atlantic coastlines which move eastwards along the Atlantic storm track where they go under explosive deepening giving rise to a more longer lifetime of the system. Concerning the duration in the Pacific, the prevalence of the long-lasting systems in the western area is likely associated with a wider ocean surface where these systems move and deepen with respect to, for example, the systems originated in Eastern Pacific and becoming explosive there.

Figure 9 shows the relative frequency of ECs in each area selected in the three categories related to $MSLP_{min}$ (a), DR_{max} (b), ADR_{max}(c), NDR_{cmax} (d). Deeper systems ($MSLP_{min}$[75p,100p]) (a) are more frequent in the Atlantic: a total 57% of ECs in the WATL and 65% of ECs in the EATL are found there with respect to the 46% of ECs observed in the WPAC and 49% of ECs observed in the EPAC. This result is in agreement with previous works (Wang and Rogers, 2001; Trigo 2006; Raible, 2007) which observed that extreme cyclones are more frequent in the eastern part of the Atlantic and are linked to temperature gradient between 300 and 700 hPa between Greenland and Northern Europe which increases the baroclinicity and thus the cyclone intensity in the area (Raible, 2007). Shallower systems ($MSLP_{min}$[0p,50p]) are prevalent in the Pacific: about the 26% of ECs detected in WPAC and 23% found in EPAC with respect to the 21% of systems found in the WATL and 16% found in EATL. The frequencies values observed are statistically different in the western parts of the basin (WATL/WPAC) and the Atlantic (WATL/EATL). Still the differences observed in the frequency values (23/29% and 19/29%) of intermediate category ($MSLP_{min}$[50p,75p]) between the western and eastern parts of both basins (WATL/WPAC and EATL/EPAC) are again statistically significant.

High deepening rates (DR_{max}, DR_{max}[75p,100p]) (b) are detected more frequently in the Atlantic region (30% of ECs in WATL and 33% of ECs in the EATL) with respect to the Pacific Area (19% of ECs in both WPAC and EPAC), where lower values of deepening rate (DR_{max}[0p,50p]) are more likely to be observed in the Pacific with overall frequency of ECs in WPAC and EPAC equal, respectively, to 56% and 58%. The last category in the Atlantic region shows a minimum of frequency equal to 45% in WATL and 36% in EATL. These differences observed are significantly different in the western/eastern part of the basins (WATL/WPAC and EATL/EPAC) while in the Atlantic region (WATL/EATL) a statistical significant signal has been observed for the category DR_{max}[0p,50p] and for the couple EATL/EPAC for the intermediate category DR_{max}[50p,75p] with frequency values equal to 28/23%, respectively.

Concerning ADR_{max} (c) 29% of ECs detected in the WATL and 27% of ECs detected in the EATL belong to ADR_{max}[75p,100p] with respect to the 25% of ECs observed in the WPAC and 18% of ECs in EPAC. Lower ADR_{max} are observed more frequently in the Pacific (50% in WPAC and 55% in EPAC) with respect to the Atlantic (46% in WATL and 50% in EATL). No significant differences have been observed in the Atlantic (despite for the aforementioned categories the values of statistical tests are very close to the significative threshold). The frequency values observed are statistically different in the Pacific (WPAC/EPAC) and in the western(WATL/WPAC) and eastern part (EATL/EPAC) of both basins.

Finally higher NDR_{cmax} (d) are observed more frequently in the western part of both basins. In fact the

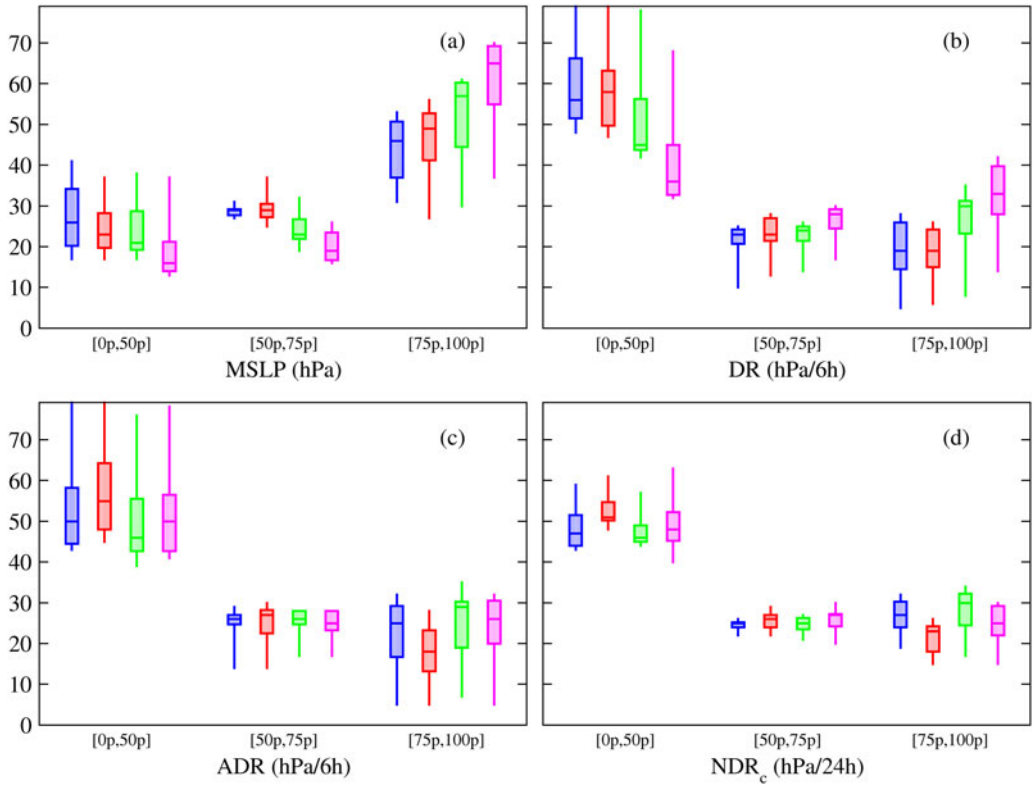

Fig. 9. Same as Fig. 8 for $MSLP_{min}$(a), DR_{max}(b), ADR_{max}(c) and NDR_{cmax}(d).

overall frequency of NDR_{cmax}[75p,100p] is equal to 30% in WATL, 27% in the WPAC, 25% in the EATL and 23% in EPAC. On the other hand, lower values category is prevalent in the eastern part of both basins with an overall relative frequency of 51% in EPAC and 48% in EATL with respect to 46% observed in WATL and 47% observed in the WPAC. No significant statistical signals have been observed comparing the eastern part of both basins (EATL/EPAC) while the frequency values observed are statistically different for the category NDR_{cmax}[75p,100p] for the western parts of both basins (WATL/WPAC) and in the Atlantic region (WATL/EATL, Wang and Rogers, 2001). In the Pacific the frequency values observed for the two targeted areas are statistically different for both NDR_{cmax}[75p,100p] and NDR_{cmax}[0p,50p] categories.

3.4.2. Southern hemisphere. For the SH (Fig. 7b) we followed in the regional analysis the same approach introduced in the previous section. First, we choose three areas satisfying the criteria listed in the introduction of Section 3.4: SAME (southern South America, red), SAFR (Southern Africa, blue) and AUST (Australia, green) (Fig. 7b). Second, we assessed the sensitivity of the relative frequency of ECs in function of the metrics considered with respect to a shift from one degree up to three degrees in the four direction previously introduced (not shown) and found no significant differences among the resulting distributions, independently from the shift of the area. An exception has been observed in the case of SAME when the shift of the area increases the fraction of land included in the domain, where (as shown Figs. 3 and 4) the level of agreement among the methods is lower giving rise to a higher dispersion among the methods.

All the ECs gathered in each category have been considered in an extended winter season AMJJASO. This period accounts for more than 70% of ECs detected SH (see Section 3.1) and so again it can be considered quite representative of ECs activity in the SH. In the period AMJJASO 1979–2008 an average number per year of 27 ± 9 ECs have been detected in SAFR, 19 ± 4 in SAME, 22 ± 8 in AUST. Thus the highest number of ECs is observed close to Southern Africa, followed by AUST and SAME; this independently of the size of the areas chosen which are quite different (74502.88 km^2 for SAME, 70363.84 km^2 for SAFR and 84850.47 km^2 for AUST). Nevertheless most of ECs becoming explosive in SAFR are originated close to Southern America (not

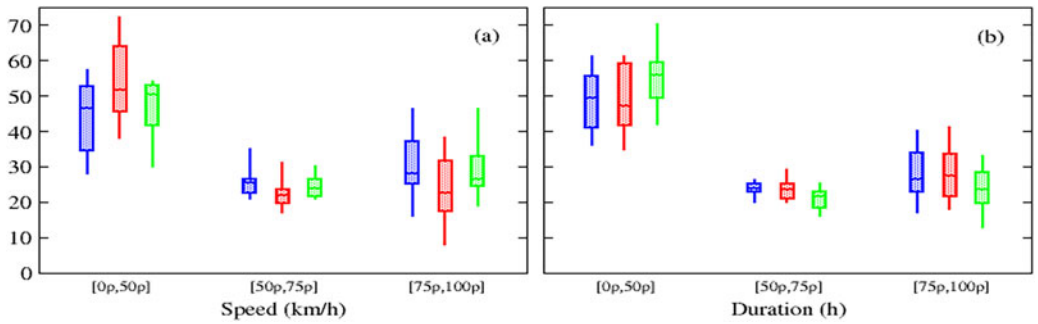

Fig. 10. Same as Fig. 8 but for SAFR (blue), SAME (red) and AUST (green).

shown) confirming that western Southern American continental coastlines are the areas where cyclogenesis processes are more frequent in the SH (e.g. Lim and Simmonds, 2002; Allen et al.,2010; Neu et al., 2013). No significant tendencies have been observed in MCDTM in these areas according to MK.

Figure 10(a,b) shows the relative frequency of ECs in SAME, SAFR and AUST gathering according to $speed_{max}$ (a) and duration (b). Faster systems ($speed_{max}$[75p,100p]) are more frequent in SAFR (28% of ECs detected here) and in AUST (26.5%). SAME shows lower frequency values (22%) for this category and a maximum frequency value of 51.5% for $speed_{max}$[0p,50p] with respect to 50.5% and 46.5% observed, respectively, observed in AUST and SAFR. The frequency values of both categories are resulted to be statistically different comparing SAME/SAFR and for the category $speed_{max}$[75p,100p] in the case of the couple SAME/AUST. Long-lasting system ECs (DURATION[75p,100p])) are prevalent in SAME (27.5% of EC detected) and in SAFR (26.5%) with respect to the 23.5% of ECs observed in AUST where short lasting systems (DURATION[0p,50p]) are prevalent (56%). The only statistical significant difference for the frequency values have been observed comparing both categories in the case of the couple SAFR/AUST and for the couple SAME/AUST in the case of the category DURATION[0p,50p].

So while in the case of SAME/SAFR ECs tend to last more probably because once they formed, they travel greater distance due to interaction with the ocean below following the spiral path observed in Fig. 3(b) in the case of $speed_{max}$ the higher baroclinicity of SAFR and AUST associated with Circumpolar current and the position with respect to the Antarctica (Lim and Simmonds, 2002) result in faster ECs with respect to SAME.

Figure 11 shows the relative frequency of ECs in the three categories related to $MSLP_{min}$ (a), DR_{max} (b), ADR_{max}(c), NDR_{cmax} (d). Deeper systems (a, $MSLP_{min}$[75p,100p]) are observed more frequently in SAFR (52.5%) and AUST (51.5%) with respect to SAME (33.5%) where, on the other hand, shallower systems ($MSLP_{min}$[0p,50p])) are more common (37.5% of ECs detected there). The latter is almost the double of the frequencies values observed in SAFR and AUST (19.5% and 21%, respectively). The values observed for both categories are resulted to be statistically different comparing SAME and SAFR and SAME and AUST. The differences observed are likely to be a consequence of more pronounced baroclinicity of the areas falling in the domain SAFR and AUST with respect to SAME. In fact these areas are characterised by significant SST gradients linked to Circumpolar Antarctic current and characterised by katabatic outflow from the Antarctica towards the ocean which give rise to more intense EC in the area (Lim and Simmonds, 2002).

High values of DR_{max} (b,DR_{max}[75p,100]) are prevalent in SAFR with a frequency approximately of 27% with respect to the value of 24,5% observed in both SAME and AUST. The intermediate category (DR_{max}[50p,75p]) is prevalent in AUST and SAFR (28%) with respect to SAME (23.5%). Finally DR_{max}[0p,50p] shows higher frequency value in SAME (52.5%) with respect to SAFR (45.5%) and AUST (47.5%). The frequency values related to DR_{max}[50p,75p] and DR_{max}[0p,50p] are statistically different when we compare SAME and SAFR and SAME and AUST. Concerning ADR_{max}(c), ADR_{max}[75p,100p] systems are more frequent in SAME (36%) with respect to SAFR (24.5%) and AUST (24%) while the systems belonging to ADR_{max}[0p,50p] are more frequent in AUST (53%) with respect to SAFR (49%) and SAME (34.5%). The frequency value observed in both categories are resulted to be statistically different comparing SAME and SAFR and SAME and AUST. So while DR_{max} is higher for SAFR and AUST, the opposite situation takes place in the case of ADR_{max} reflecting a more probable equatorward location for the maximum deepening in SAME with respect to the same process taking place in SAFR and AUST.

Finally for NDR_{cmax} (d), NDR_{Cmax}[75p,100p] are observed more frequently in SAME (31.5%) and SAFR (30%) with respect to AUST(20%). On the other hand,

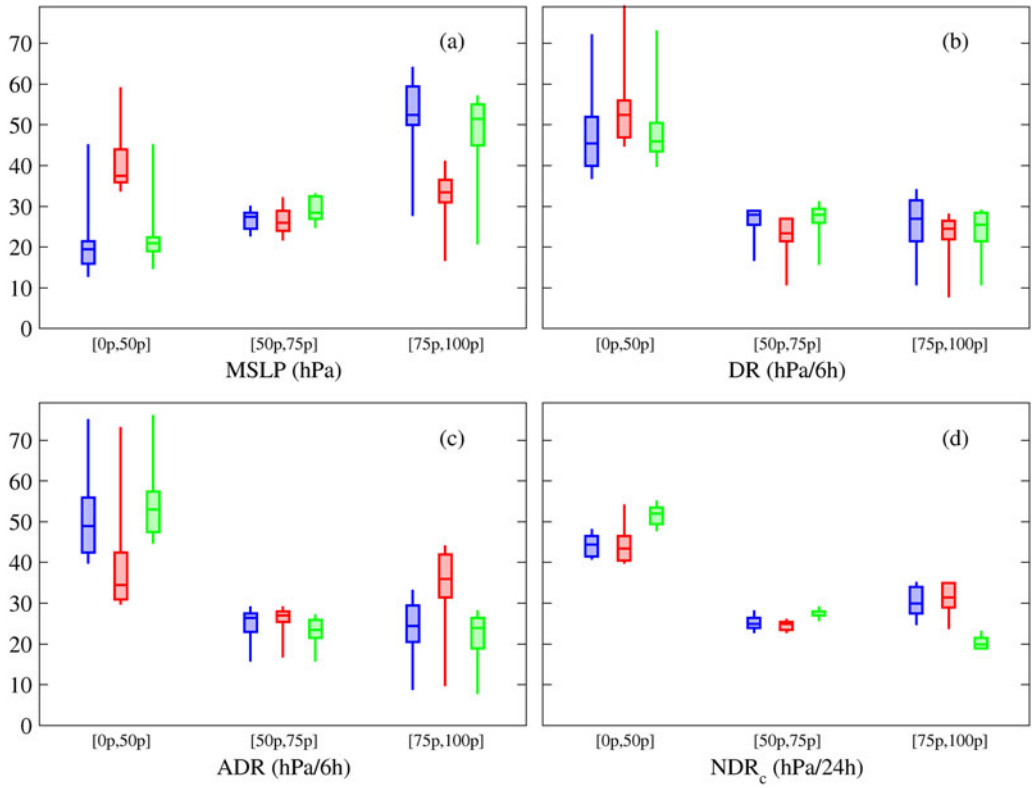

Fig. 11. Same as Fig. 9 but for SAFR (blue), SAME (red) and AUST (green).

NDR_{Cmax}[0p,50p] are more frequent in the AUST with an overall relative frequency of 52% with respect to the 44.5% observed in SAFR and 43.5% in SAME. While no statistically significant differences have been observed comparing SAME and SAFR the frequency values observed have been resulted to be statistically different for both categories comparing SAME and AUST and SAFR and AUST. Again with respect to the physical forcing as air-sea interaction these findings are likely to be more linked to the location of the areas chosen for the analysis. As shown in Fig. 4(d), the explosive developments in the case of SAME and SAFR are likely to occur more frequently equatorward with respect to AUST where it may take place in a more poleward location.

4. Summary and conclusions

In this paper we have described and discussed the climatology of ECs for both hemispheres using the multi CDTMs approach (e.g. Neu et al., 2013). This approach enables to capture the main characteristics of ECs activity in both hemispheres despite the differences among CDTMs in detecting and tracking each system. Despite the huge spread in the number of ECs identified by each CDTM (up to 21% and 38% in the NH and SH, respectively) the methods agree on the areas where the explosive activity is more prominent and confirm previous studies (e.g. Allen et al., 2010; Seiler and Zwiers, 2016): the eastern North American Coastlines, Japanese Coastlines, the area east off the Southern American coastlines and the area around the Antarctica. ECs activity is high during the cold season in both hemispheres, in particular in January (NH) and July (SH), though seasonality is lower in the SH than in the NH.

In both hemispheres, ECs tend to be deeper, faster and long lasting with respect to NECs. In particular, in both hemispheres the SLP minimum of ECs is on the average 20 hPa lower than in NECs, the deepening rate over 6 h is double and the normalised deepening rate over 24 h is usually eight times larger than the value in NECs. In the SH, ECs are deeper and slightly last longer than their NH counterparts. On the other hand, when considering DR_{max}, ADR_{max}, and NDR_{cmax} ECs in the NH are characterised by a larger rate of central pressure decrease during their deepening than in the SH. No striking differences have been identified between the two hemispheres in term of EC $speed_{max}$.

In the NH, ECs are usually faster, deeper and with higher DR_{max} and ADR_{max} in the Atlantic than in the Pacific, particularly in the eastern part of the basin. In both oceans, ECs NDR_{cmax} is higher in the western areas

than in the eastern areas. In fact, in the western areas of the oceans the explosive processes are strongest, as they are characterised by strong horizontal SST gradients (Lim and Simmonds, 2002; Allen et al., 2010; Neu et al., 2013; Seilers and Zwiers, 2016) and strong air-sea interaction, which fuels explosive developments. These differences are statistically significant in particular comparing Western Atlantic to Western Pacific and Eastern Atlantic to Eastern Pacific (for $MSLP_{min}$, DR_{max}, ADR_{max}, $speed_{max}$), and comparing Western Atlantic to Eastern Atlantic (for the $MSLP_{min}$). On this respect, the ECs in the four areas, at least for the extreme categories, can be considered as belonging to the different populations.

In the SH, ECs close to Southern Africa and Australia are usually faster, deeper and with higher DR_{max} with respect to those close to southern South America, and ECs close to southern South America and Southern Africa are characterised by higher $NDRC_{max}$ and duration with respect to ECs close to Australia. Also these differences are statistically significant in particular for the extreme categories, showing that for the metrics chosen these systems can be considered as belonging to different populations.

This work has confirmed the importance of multi CDTMs approach in identifying and characterising cyclone activity, because of prominent differences among the methods.

NOTES

1. $\frac{\sigma}{\mu}$ where σ is the standard deviation and μ is the mean
2. https://newonlinecourses.science.psu.edu/stat414/node/268/

Acknowledgments

MR is grateful to European Meteorological Society for its Young Scientist Travel Awards and for allowing the author to attend the EMS meeting in Dublin in September 2017. JGP thanks the AXA research fund for support.

Funding

This work was supported by OGS and CINECA under HPC-TRES program [grant number 2015-07 to MR]; the project WEx-Atlantic [grant number PTDC/CTA-MET/29233/2017 to MLRL]; and Instituto Dom Luiz funded by Fundação para a Ciência e a Tecnologia, Portugal (FCT) and Portugal Horizon 2020 [grant number UID/GEO/50019/2013].

References

Allen, J. T., Pezza, A. B. and Black, M. T. 2010. Explosive cyclogenesis: a global climatology comparing multiple reanalyses. *J. Clim.* **23**, 6468–6484. doi:10.1175/2010JCLI3437.1

Akperov, M. G., Bardin, M. Y., Volodin, E. M., Golitsyn, G. S. and Mokhov, I. I. 2007. Probability distributions for cyclones and anticyclones from the NCEP/NCAR reanalysis data and the INM-RAS climate model. *Izvestiya. Atmos. Ocean. Phys.* **43**, 705–712. doi:10.1134/S0001433807060047

Bardin, M. Y. and Polonsky, A. B. 2005. North Atlantic oscillation and synoptic variability in the European-Atlantic region in winter, Izvestiya. *Atmos. Ocean. Phys.* **41**, 127–136.

Chang, E. K., Lee, S. and Swanson, K. L. 2002. Storm track dynamics. *J Clim* **15**, 2163–2183.

Chen, S. J., Kuo, Y. H., Zhang, P. Z. and Bai, Q. F. 1992. Climatology of explosive cyclones off the east Asian coast. *Mon. Wea. Rev.* **120**, 3029–3035. doi:10.1175/1520-0493(1992)120<3029:COECOT>2.0.CO;2

De Zolt, S., Lionello, P., Malguzzi, P., Nuhu, A. and Tomasin, A. 2006. The disastrous storm of 4 November 1966 on Italy. *Nat. Hazards. Earth. Syst. Sci.* **6**, 861–879. doi:10.5194/nhess-6-861-2006

Flaounas, E., Kelemen, F. D., Wernli, H., et al. 2016. Assessment of an ensemble of ocean–atmosphere coupled and uncoupled regional climate models to reproduce the climatology of Mediterranean cyclones. *Clim. Dyn.* **51**, 1023–1040.

Fink, A. H., Brücher, T., Ermert, V., Krüger, A. and Pinto, J. G. 2009. The European storm Kyrill in January 2007: Synoptic evolution and considerations with respect to climate change. *Nat. Hazards Earth Syst. Sci.* **9**, 405–423. doi:10.5194/nhess-9-405-2009

Fink, A. H., Pohle, S., Pinto, J. G. and Knippertz, P. 2012. Diagnosing the influence of diabatic processes on the explosive deepening of extratropical cyclones. *Geophys. Res. Lett.* **39**, L07803.1–L07803.8.

Gómara, I., Rodríguez-Fonseca, B., Zurita-Gotor, P. and Pinto, J. G. 2014. On the relation between explosive cyclones affecting Europe and the North Atlantic Oscillation. *Geophys. Res. Lett.* **41**, 2182–2190. doi:10.1002/2014GL059647

Gyakum, J. R., Anderson, J. R., Grumm, R. H. and Gruner, E. L. 1989. North Pacific cold-season surface cyclone activity: 1975–1983. *Mon. Wea. Rev.* **117**, 1141–1155. doi:10.1175/1520-0493(1989)117<1141:NPCSSC>2.0.CO;2

Grieger, J., Leckebusch, G., C., Raible, C., Rudeva, I. and Simmonds, I. 2018. Subantarctic cyclones identified by 14 tracking methods, and their role for moisture transports into the continent. *Tellus A: Dynamic Meteorology and Oceanography* **70**, 1. doi:10.1080/16000870.2018.1454808

Hewson, T. D. 1997. Objective identification of frontal wave cyclones. *Meteorol. App.* **4**, 311–315. doi:10.1017/S135048279700073X

Hewson, T. D. and Titley, H. A. 2010. Objective identification, typing and tracking of the complete life-cycles of cyclonic features at high spatial resolution. *Met. Apps.* **17**, 355–381. doi:10.1002/met.204

Hewson, T. and Neu, U. 2015. Cyclones, windstorms and the IMILAST project. *Tellus A: Dynamic Meteorology and Oceanography* **67**, 27128. doi:10.3402/tellusa.v67.27128

Hoskins, B. and Hodges, K. 2005. A new perspective on Southern Hemisphere storm tracks. *J. Climate*, **18**, 4108–4129.

Kouroutzoglou, J., Flocas, H. A., Keay, K., Simmonds, I. and Hatzaki, M. 2011. Climatological aspects of explosive cyclones in the Mediterranean. *Int. J. Climatol.* **31**, 1785–1802. doi:10.1002/joc.2203

Kuwano-Yoshida, A. and Asuma, Y. 2008. Numerical study of explosively developing extratropical cyclones in the Northwestern Pacific region. *Mon. Wea. Rev.* **136**, 712–740. doi:10.1175/2007MWR2111.1

Kuwano-Yoshida, A. and Enomoto, T. 2013. Predictability of Explosive Cyclogenesis over the Northwestern Pacific Region Using Ensemble Reanalysis. *Mon. Wea. Rev.* **141**, 3769–3785. doi:10.1175/MWR-D-12-00161.1

Liberato, M. L. R., Pinto, J. G., Trigo, I. F. and Trigo, R. M. 2011. Klaus – an exceptional winter storm over northern Iberia and southern France. *Weather* **66**, 330–334. doi:10.1002/wea.755

Liberato, M. L. R. 2014. The 19 January 2013 windstorm over the North Atlantic: large-scale dynamics and impacts on Iberia. *Weather Clim. Extremes* **5**, 16–28.

Lim, E. and Simmonds, I. 2002. Explosive cyclone development in the Southern Hemisphere and a comparison with Northern Hemisphere events. *Mon. Wea. Rev.* **130**, 2188–2209. doi:10.1175/1520-0493(2002)130<2188:ECDITS>2.0.CO;2

Lionello, P., Dalan, F. and Elvini, E. 2002. Cyclones in the Mediterranean region: the present and the doubled CO2 climate scenarios. *Clim. Res.* **22**, 147–159. doi:10.3354/cr022147

Lionello, P. et al. 2016. Objective climatology of cyclones in the Mediterranean region: a consensus view among methods with different system identification and tracking criteria. *Tellus: Series A, Dynamic Meteorology and Oceanography*, **68**, 1–18.

Ludwig, P., Pinto, J. G., Reyers, M. and Gray, S. L. 2014. The role of anomalous SST and surface fluxes over the southeastern North Atlantic in the explosive development of windstorm Xynthia. *Qjr. Meteorol. Soc.* **140**, 1729–1741. doi:10.1002/qj.2253

Murray, R. J. and Simmonds, I. 1991. A numerical scheme for tracking cyclone centers from digital data. Part I: development and operation of the scheme. *Aust. Meteorol. Mag* **39**, 155–166.

Neu, U., Akperov, M. G., Bellenbaum, N., Benestad, R., Blender, R. et al. 2013. IMILAST-a community effort to intercompare extratropical cyclone detection and tracking algorithms: assessing method-related uncertainties. *Bull. Amer. Meteor. Soc.* **94**, 529–547. doi:10.1175/BAMS-D-11-00154.1

Nissen, K. M., Leckebusch, G. C., Pinto, J. G., Renggli, D., Ulbrich, S. et al. 2010. Cyclones causing wind storms in the Mediterranean: characteristics, trends and links to largescale patterns. *Nat. Hazards Earth Syst. Sci.* **10**, 1379–1391. doi:doi:10.5194/nhess-10-1379-2010

Peixoto, J. P. and Oort, A. H. 1992. *Physics of Climate*. Springer, Berlin.

Pinto, J. G., Spangehl, T., Ulbrich, U. and Speth, P. 2005. Sensitivities of a cyclone detection and tracking algorithm: individual tracks and climatology. *Metz.* **14**, 823–838. doi:10.1127/0941-2948/2005/0068

Pinto, J. G., Ulbrich, S., Parodi, A., Rudari, R., Boni, G. et al. 2013. Identification and ranking of extraordinary rainfall events over Northwest Italy: the role of Atlantic moisture. *J. Geophys. Res. Atmos.* **118**, 2085–2097. doi:10.1002/jgrd.50179

Pinto, J. G., Ulbrich, S., Economou, T., Stephenson, D. B., Karremann, M. K. et al. 2016. Robustness of serial clustering of extratropical cyclones to the choice of tracking method. *Tellus A: Dynamic Meteorology and Oceanography* **68**, 32204. doi:10.3402/tellusa.v68.32204

Raible, C. C. 2007. On the relation between extremes of mid altitude cyclones and the atmospheric circulation using ERA40. *Geophys. Res. Lett.*, **34**, L07703.1–L07703.6

Roebber, P. J. 1984. Statistical analysis and updated climatology of explosive cyclones. *Mon. Wea. Rev.* **112**, 1577–1589. doi:10.1175/1520-0493(1984)112<1577:SAAUCO>2.0.CO;2

Rudeva, I., Gulev, S. K., Simmonds, I. and Tilinina, N. 2014. The sensitivity of characteristics of cyclone activity to identification procedures in tracking algorithms. *Tellus A* **66**, 24961. doi:10.3402/tellusa.v66.24961

Reale, M. and Lionello, P. 2013. Synoptic climatology of winter intense precipitation events along the Mediterranean coasts. *Nat. Hazards Earth Syst. Sci.* **13**, 1707–1722. doi:10.5194/nhess-13-1707-2013

Sanders, F. and Gyakum, J. R. 1980. Synoptic-dynamic climatology of the bomb. *Mon. Wea. Rev.* **108**, 1589–1606. doi:10.1175/1520-0493(1980)108<1589:SDCOT>2.0.CO;2

Sanders, F. 1986. Explosive cyclogenesis in the west-central North Atlantic Ocean, 1981-84. Part I: Composite structure and mean behavior. *Mon. Wea. Rev.* **114**, 1781–1794. doi:10.1175/1520-0493(1986)114<1781:ECITWC>2.0.CO;2

Seiler, C. and Zwiers, F. W. 2016. How well do CMIP5 climate models reproduce explosive cyclones in the extratropics of the Northern Hemisphere? *Clim. Dyn.* **46**, 1241. doi:10.1007/s00382-015-2642-x

Serreze, M. C. 1995. Climatological aspects of cyclone development and decay in the Arctic. *Atmos. Ocean* **33**, 1–23. doi:10.1080/07055900.1995.9649522

Stull, R. B. 2000. *Meteorology for Scientists and Engineers: A Technical Companion Book with Ahrens' Meteorology Today*, Pacific Grove,CA: Brooks/Cole.

Simmonds, I., Burke, C. and Keay, K. 2008. Arctic climate change as manifest in cyclone behavior. *J. Clim.* **21**, 5777–5796. doi:10.1175/2008JCLI2366.1

Trigo, I. F. 2006. Climatology and interannual variability of storm tracks in the Euro-Atlantic sector: a comparison between ERA- 40 and NCEP/NCAR reanalyses. Clim. *Clim. Dyn.* **26**, 127–143. doi:10.1007/s00382-005-0065-9

Ulbrich, U., Leckebusch, G. C., Grieger, J., et al. 2013. Are Greenhouse Gas Signals of Northern Hemisphere winter extra-tropical cyclone activity dependent on the identification and tracking algorithm? *Meteor. Z.* **22**, 61–68. doi:10.1127/0941-2948/2013/0420

Wang, X. L., Swail, V. R. and Zwiers, F. W. 2006. Climatology and changes of extra-tropical cyclone activity: comparison of ERA-40 with NCEP/NCAR reanalysis for 1958-2001. *J. Clim.* **19**, 314–3166.

Wang, C. and Rogers, J. C. 2001. A composite study of explosive cyclogenesis in different sectors of the north Atlantic. Part i: cyclone structure and evolution. *Mon. Wea. Rev.* **129**, 1481–1499. doi:10.1175/1520-0493(2001)129<1481:ACSOEC>2.0.CO;2

Wernli, H. and Schwierz, C. 2006. Surface cyclones in the ERA-40 data set (1958-2001). Part I: novel identification method and global climatology. *J. Atmos. Sci.* **63**, 2486–2507. doi:10.1175/JAS3766.1